



## ORIGINAL ARTICLE

# Role of the kringle-like domain in glycoprotein NMB for its tumorigenic potential

Rudy Xie<sup>1,2</sup> | Yukari Okita<sup>1,3</sup>  | Yumu Ichikawa<sup>1,2</sup> | Muhammad Ali Fikry<sup>1,2</sup> |  
Kim Tuyen Huynh Dam<sup>1,2</sup> | Sophie Thi PhuongDung Tran<sup>1,4</sup> | Mitsuyasu Kato<sup>1,3</sup> 

<sup>1</sup>Department of Experimental Pathology, Faculty of Medicine, University of Tsukuba, Tsukuba, Japan

<sup>2</sup>Graduate School of Comprehensive Human Sciences, University of Tsukuba, Tsukuba, Japan

<sup>3</sup>Division of Cell Dynamics, Transborder Medical Research Center, University of Tsukuba, Tsukuba, Japan

<sup>4</sup>Human Biology, School of Integrative and Global Majors, University of Tsukuba, Tsukuba, Japan

## Correspondence

Yukari Okita, Department of Experimental Pathology, Faculty of Medicine, University of Tsukuba, Tsukuba, Japan.  
Email: yukari-okita@md.tsukuba.ac.jp

## Funding information

Uehara Memorial Foundation; Japan Society for the Promotion of Science, Grant/Award Number: JP15K29070, JP17K14981 and JP18H02676

## Abstract

Glycoprotein NMB (GPNMB) is highly expressed in many types of malignant tumors and thought to be a poor prognostic factor in those cancers, including breast cancer. Glycoprotein NMB is a type IA transmembrane protein that has a long extracellular domain (ECD) and a short intracellular domain (ICD). In general, the ECD of a protein is involved in protein-protein or protein-carbohydrate interactions, whereas the ICD is important for intracellular signaling. We previously reported that GPNMB contributes to the initiation and malignant progression of breast cancer through the hemi-immunoreceptor tyrosine-based activation motif (hemITAM) in its ICD. Furthermore, we showed that the tyrosine residue in hemITAM is involved in induction of the stem-like properties of breast cancer cells. However, the contribution of the ECD to its tumorigenic function has yet to be fully elucidated. In this study, we focused on the region, the so-called kringle-like domain (KLD), that is conserved among species, and made a deletion mutant, GPNMB( $\Delta$ KLD). Enhanced expression of WT GPNMB induced sphere and tumor formation in breast epithelial cells; in contrast, GPNMB( $\Delta$ KLD) lacked these activities without affecting its molecular properties, such as subcellular localization, Src-induced tyrosine phosphorylation at least in overexpression experiments, and homo-oligomerization. Additionally, GPNMB( $\Delta$ KLD) lost its cell migration promoting activity, even though it reduced E-cadherin expression. Although the interaction partner binding to KLD has not yet been identified, we found that the KLD of GPNMB plays an important role in its tumorigenic potential.

## KEYWORDS

epithelial-mesenchymal transition, GPNMB, kringle-like domain, sphere formation, tumorigenicity

**Abbreviations:** ECD, extracellular domain; EEA1, early endosome antigen 1; EGF, epidermal growth factor; EMT, epithelial-mesenchymal transition; GPNMB, glycoprotein NMB; ICD, intracellular domain; ITAM, immunoreceptor tyrosine-based activation motif; KD, kringle domain; KLD, kringle-like domain; LAMP1, lysosome-associated membrane protein 1; MuSK, muscle-specific receptor tyrosine kinase; NMB, nonmetastatic melanoma protein B; PCP, planar cell polarity; PKD, polycystic kidney disease; PMEL, premelanosome protein; RGD, arginyl-glycyl-aspartic acid; ROR, receptor tyrosine-like orphan receptor.

This is an open access article under the terms of the Creative Commons Attribution-NonCommercial License, which permits use, distribution and reproduction in any medium, provided the original work is properly cited and is not used for commercial purposes.

© 2019 The Authors. *Cancer Science* published by John Wiley & Sons Australia, Ltd on behalf of Japanese Cancer Association.

## 1 | INTRODUCTION

Glycoprotein NMB is a type IA transmembrane protein that is highly expressed in many types of cancers, including melanoma, glioblastoma, and breast cancer. It is considered a poor prognostic factor in those cancers and it might be an attractive therapeutic target.<sup>1-5</sup>

We have previously reported that enhanced expression of GPNMB induces EMT and increases sphere formation in vitro and tumor growth in vivo, whereas knockdown of GPNMB attenuated the tumorigenic ability of breast cancer cells.<sup>6</sup> We also showed that cell surface expression of GPNMB is induced in limited numbers of breast cancer cells in sphere-culture conditions in vitro and in growing tumors in vivo and induces stem-like properties, such as high expression of stemness genes, low expression of proliferation genes, and high sphere and tumor formation.<sup>7</sup> These functions depend on the tyrosine residue of the hemITAM in the ICD of GPNMB.<sup>6,7</sup> In addition, Lin et al<sup>8</sup> reported that GPNMB interacts with epidermal growth factor receptor and that stimulation of heparin-binding EGF triggers the phosphorylation of the tyrosine residue in hemITAM. They also showed the significance of tyrosine phosphorylation in the poorer prognosis of breast cancer patients. These findings together with ours suggest that both the ICD and the ECD are essential for the tumorigenic function of GPNMB; however, the function of the ECD has yet to be fully elucidated.

Glycoprotein NMB consists of a long ECD that contains an N-terminal signal peptide, an RGD motif, a PKD domain, and a KLD, a single-pass transmembrane domain, and a short ICD that harbors a hemITAM and a dileucine motif.<sup>2,9-11</sup> The RGD motif is known as an integrin-binding sequence and has been shown to be involved in the migratory activity of breast cancer cells<sup>12</sup> and cell-cell adhesion.<sup>13,14</sup> Glycoprotein NMB interacts with syndecan-4, which is expressed on the surface of T cells, through the PKD, and this interaction suppresses T-cell activation and proliferation.<sup>15-19</sup> So far, little is known about the function of the KLD in GPNMB. Therefore, in the present study, we clarified the contribution of the KLD to the tumorigenic function of GPNMB.

## 2 | MATERIALS AND METHODS

### 2.1 | Cells and cell culture

293T cells and NMuMG cells were obtained from the ATCC. We cultured these cells in DMEM (Sigma-Aldrich) supplemented with 10% FBS, 100 units/mL penicillin G, and 0.1 mg/mL of streptomycin sulfate (Wako Pure Chemical Industries). NMuMG cells stably expressing GPNMB, both WT and KLD-deletion mutant ( $\Delta$ KLD), were maintained in the presence of puromycin (1  $\mu$ g/mL; Sigma-Aldrich).<sup>6</sup> L Wnt-3A cells and L cells (ATCC) were used to prepare Wnt3A conditioned medium and control medium as described previously.<sup>20</sup>

### 2.2 | DNA constructs and transfection

Glycoprotein NMB and Src cDNA were cloned previously,<sup>6</sup> and GPNMB( $\Delta$ KLD) lacking amino acids 420-491 of mouse GPNMB

was generated by PCR, followed by cloning into pCAGIP- or pcDEF3-expressing vectors. pCAG-GS- $\beta$ -catenin and TOP-flash luciferase reporter were described previously.<sup>20</sup> These constructs were transfected into cells by use of PEI Max (Polysciences). To establish stably expressing cell lines, NMuMG cells were transfected using Lipofectamine 3000 (Invitrogen) as described previously.<sup>6,21</sup>

### 2.3 | Immunoprecipitation

For the immunoprecipitation, 293T cells were transfected with the indicated plasmids, and the cells were then solubilized in lysis buffer (20 mmol/L Tris-HCl, pH 7.5, 150 mmol/L NaCl, 1% Nonidet P-40, 2000 kIU/mL aprotinin, and 1  $\mu$ g/mL leupeptin). The debris was then precipitated by centrifugation; a small amount of total cell lysates was collected and the remainder was used for immunoprecipitation with anti-FLAG Ab (M2; Sigma-Aldrich).

### 2.4 | Sodium dodecyl sulfate-PAGE and immunoblot analysis

The protein samples were subjected to SDS-PAGE. The proteins were then electrotransferred to PVDF membranes (Millipore) and subjected to immunoblot analysis. Antibodies against FLAG (M2; Sigma-Aldrich), HA (3F10; Roche Diagnostics), c-Myc (9E10; Santa Cruz Biotechnology), and phosphorylated tyrosine (4G10; Millipore) were used. The reacted Abs were detected as described previously.<sup>22</sup>

### 2.5 | Flow cytometry

293T cells were transfected with the indicated plasmids and treated with trypsin (Sigma) to yield single cells. The floating single cells were incubated with anti-GPNMB Ab (AF2550; R&D Systems), and then with Alexa 488-labeled donkey anti-goat IgG (Molecular Probes) on ice for 30 minutes. The samples were analyzed using a BD FACSCalibur (BD Biosciences) and BD CellQuest software (BD Biosciences).

### 2.6 | Reverse transcription-PCR and quantitative real-time PCR

Reverse transcription-PCR (RT-PCR) was carried out as described previously.<sup>23</sup> In brief, total RNA was extracted using ISOGEN II reagent (Nippon Gene). Reverse transcription was undertaken using High Capacity RNA-to-cDNA Master Mix (Applied Biosystems) and semiquantitative RT-PCR was carried out with the previously described specific primers<sup>6</sup> and using Ex Taq polymerase (Takara). Real-Time PCR was performed using GeneAmp SYBR quantitative real-time PCR (qPCR) mix  $\alpha$  Low ROX (Nippon Gene) and the ABI7500 Fast Sequence Detection system (Applied Biosystems). All samples were run in triplicate in each experiment. Primer sequences are as follows:

mouse *Axin2* forward, 5'-TGACTCTCCTTCCAGATCCCA-3', and reverse 5'-TGCCCACTAGGCTGACA-3'); and mouse  $\beta$ -actin forward, 5'-CGATGCCCTGAGGCTCTTT-3', and reverse 5'-TGGATGCCACAGGATTCCA-3'.

## 2.7 | Sphere formation

A total of  $5 \times 10^3$  NMuMG-mock, NMuMG-GPNMB(WT), or NMuMG-GPNMB( $\Delta$ KLD) cells were cultured in DMEM/F12 medium (Sigma-Aldrich) supplemented with 20  $\mu$ L/mL B27 (Invitrogen), 20 ng/mL EGF (Sigma-Aldrich), and 20 ng/mL basic fibroblast growth factor (Wako Pure Chemical Industries) in each ultra-low attachment culture dish (35 mm; Corning). The size of the spheres was measured and the number of the spheres was counted on day 7.

## 2.8 | Tumor formation

A total of  $1 \times 10^7$  NMuMG-mock, NMuMG-GPNMB(WT), or NMuMG-GPNMB( $\Delta$ KLD) cells were injected s.c. into 6-week-old female ICR-*nu/nu* mice (Clea Japan). The mice were killed, and the tumor grafts harvested at 8 weeks postinjection. The tumor volumes were approximated using the following formula: volume =  $0.5 \times a \times b^2$ , in which *a* and *b* are the lengths of the major and minor axes, respectively. The tumors were then fixed in phosphate-buffered formalin solution and embedded in paraffin, and the sections were subjected to H&E staining and immunohistochemistry. All animal experiments were carried out with approval from the Animal Ethics Committee of the University of Tsukuba and in accordance with the university's animal experiment guidelines and the provisions of the 1995 Declaration of Helsinki.

## 2.9 | Transwell migration assay

A total of  $3 \times 10^4$  NMuMG-mock, NMuMG-GPNMB(WT), or NMuMG-GPNMB( $\Delta$ KLD) cells were seeded into a Transwell chamber (8- $\mu$ m pore; Corning). After 16 hours, the cells were fixed with 3.7% formaldehyde and stained with 0.5% crystal violet. Four high-power field pictures of the lower surface of each Transwell membrane were photographed under microscopic observation, and the migrated cell numbers were counted.

## 2.10 | Immunofluorescence staining

The cells were fixed in 4% paraformaldehyde. After fixation, we incubated the cells using PBS supplemented with 0.3% Triton-X and 1% BSA for cell-membrane permeabilization and blocking. The primary Abs used were against GPNMB (AF2550; R&D Systems), LAMP1 (Cell Signaling Technology), and EEA1 (Cell Signaling Technology). The reacted Abs were detected with fluorescence-conjugated anti-rabbit IgG (Alexa Fluor 568; Molecular Probes) and fluorescence-conjugated anti-goat IgG (Alexa Fluor 488;

Molecular Probes). TO-PRO3 (Thermo Fisher Scientific) was used for nuclear staining. For the actin staining, fluorescein phalloidin (Molecular Probes) was used. A confocal laser-scanning microscope, the TCS SP8 (Leica Microsystems), was used for the detection and image taking.

## 2.11 | Immunohistochemical staining

The paraffin-embedded tissue sections were deparaffinized in xylene, rehydrated in ethanol, and immersed in citrate-NaOH buffer (10 mmol/L sodium citrate, pH 6.0) at 121°C for 20 minutes. After retrieval of antigenicity, the nonspecific Ab reaction was blocked in blocking solution (PerkinElmer Life Sciences), and the samples were incubated with Abs against HA (3F10; Roche Diagnostics), E-cadherin (610181; BD Biosciences), and Ki-67 (Abcam). After the sections had been washed, the reacted Abs were detected using the Dako EnVision+ System/HRP (DAB) (DakoCytomation).

## 2.12 | Transmission electron microscopy

Fresh tissues were fixed with 2.5% glutaraldehyde in 0.1 mol/L phosphate buffer (LSI Medience) at 4°C, and after the samples had been washed 3 times with 0.1 mol/L phosphate buffer, they were postfixed in 1% OsO<sub>4</sub> for 1 hour at 4°C. After being dehydrated in a series of increasing ethanol concentrations, the samples were embedded in Epon 815 (Fujifilm). The ultrathin sections were stained with uranyl acetate and lead citrate and examined under a transmission electron microscope, the JEM-1400 (JEOL).

## 2.13 | Sequence alignment

Protein sequence information was obtained from the NCBI. The bioinformatic software Lasergene (DNASTAR) was used to analyze the homology of the sequences. The alignment results were obtained using the MegAlign program with the Jotun Hein method.

## 2.14 | Luciferase reporter assay

Cells were transfected with the TOP-flash *firefly* luciferase reporter and pRL-CMV *Renilla* luciferase reporter. Luciferase activity in cell lysates was determined by a Luciferase reporter assay system (Promega) using a luminometer (MicroLumat). Luciferase activities were normalized to corresponding *Renilla* luciferase activity.

## 2.15 | Statistical analysis

Quantitative data are expressed as mean  $\pm$  SD. The statistical analyses were undertaken using 1-way ANOVA with the Tukey multiple comparison test with GraphPad Prism 7 software (GraphPad) or Student's *t* test with Excel (Microsoft). Probability values <0.05 were considered significant.

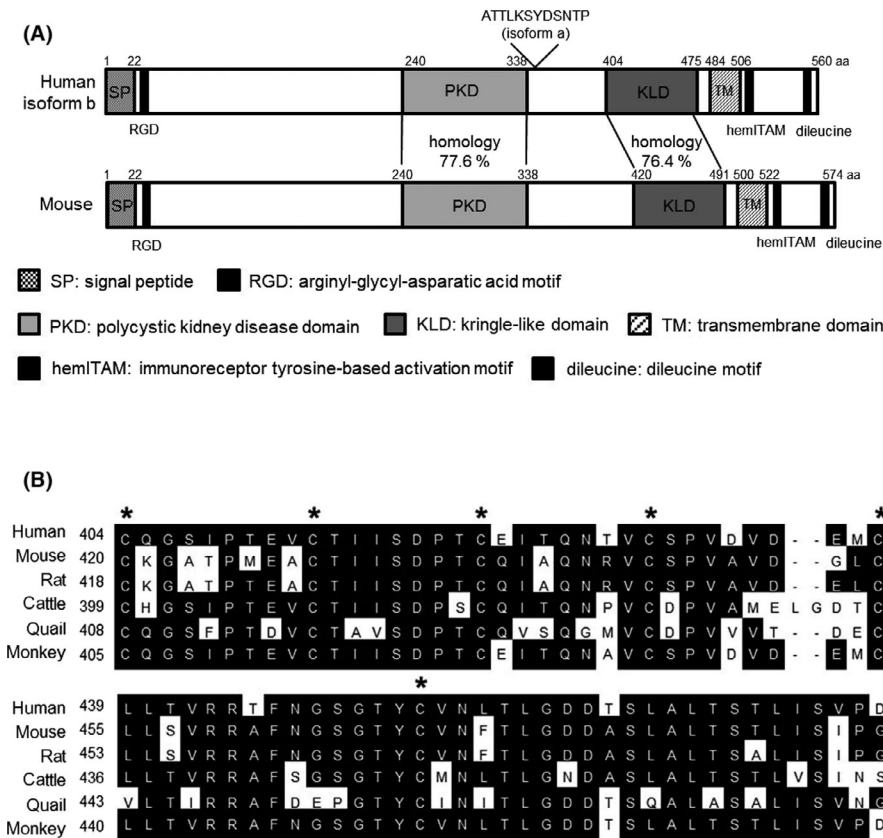


**FIGURE 1** Kringle-like domain (KLD) of glycoprotein NMB (GPNMB) is conserved among species. A, 2D scheme of human and mouse GPNMB showing the extracellular domain consisting of a signal peptide (SP), an arginyl-glycyl-aspartic acid motif (RGD), a polycystic kidney disease domain (PKD), and a KLD, the single-pass transmembrane domain (TM), and the intracellular domain consisting of a hemi-immunoreceptor tyrosine-based activation motif (hemITAM) and a dileucine motif. B, Conservation of the KLD among species. Asterisks indicate the conserved cysteines in the domain

### 3 | RESULTS

#### 3.1 | Glycoprotein NMB has a KLD that is conserved across species

To identify the important region in the ECD of GPNMB in terms of its tumorigenic potential, we reviewed its motif and domain structures (Figure 1A). Among all the known motifs and domains in the ECD, little is known about the function of the KLD, although the KLD of PMEL, a GPNMB homologous protein, promotes amyloid formation by facilitating PMEL oligomerization.<sup>24</sup> In general, a KD contains 80 amino acids and its typical loop structures are formed by 3 intramolecular disulfide bonds.<sup>24</sup> We first examined the conservation of the KLD among species and found that the KLD of GPNMB is highly conserved across species, including the 6 cysteines that are important in the disulfide bond formation in the KD (Figure 1B).

#### 3.2 | Deletion of the KLD does not affect GPNMB subcellular localization, tyrosine phosphorylation, or homo-oligomer formation

To investigate the function of the KLD in GPNMB, we constructed a deletion mutant of mouse GPNMB, GPNMB( $\Delta$ KLD) in which amino acids 420-491 are deleted (Figure 2A). After cloning into mammalian expressing vectors, we confirmed its expression in 293T cells (Figure 2B). In addition, flow cytometry analysis

revealed that both GPNMB(WT) and GPNMB( $\Delta$ KLD) proteins were similarly expressed on the surface of 293T cells when we transiently overexpressed them (Figure 2C). We next established stably expressing cell lines of either GPNMB(WT) or GPNMB( $\Delta$ KLD) using NMuMG cells: NMuMG-GPNMB(WT) clone 3 and clone 8 (here called G3 and G8<sup>6</sup>) and NMuMG-GPNMB( $\Delta$ KLD) clone 7 and clone 11 (here called  $\Delta$ KLD7 and  $\Delta$ KLD11) (Figure 2D). We next undertook immunofluorescence staining to examine the subcellular localization. GPNMB( $\Delta$ KLD) colocalized mainly with an endosome marker, EEA1, and a lysosome marker, LAMP1, as did GPNMB(WT) (Figure 2E), indicating that deletion of KLD does not affect its subcellular localization. Next, we evaluated the tyrosine phosphorylation by Src because our previous study showed that GPNMB was phosphorylated by Src on the tyrosine residue in its hemITAM.<sup>6</sup> As shown in Figure 2F, the deletion of KLD did not influence the phosphorylation of GPNMB, at least by coexpressed Src in 293T cells. We also found that GPNMB could form a homo-oligomer. Therefore, we investigated whether GPNMB( $\Delta$ KLD) can also make a homo-oligomer. Immunoprecipitation-immunoblot analysis showed that KLD is not responsible for the oligomer formation (Figure 2G). Although deletion of the whole domain sometimes results in a nonfunctional protein, these results suggest that the deletion of the KLD does not affect the basic properties of GPNMB, such as subcellular localization, tyrosine phosphorylation, and homo-oligomer formation. Therefore, we continued to investigate the tumorigenic functions of GPNMB( $\Delta$ KLD).

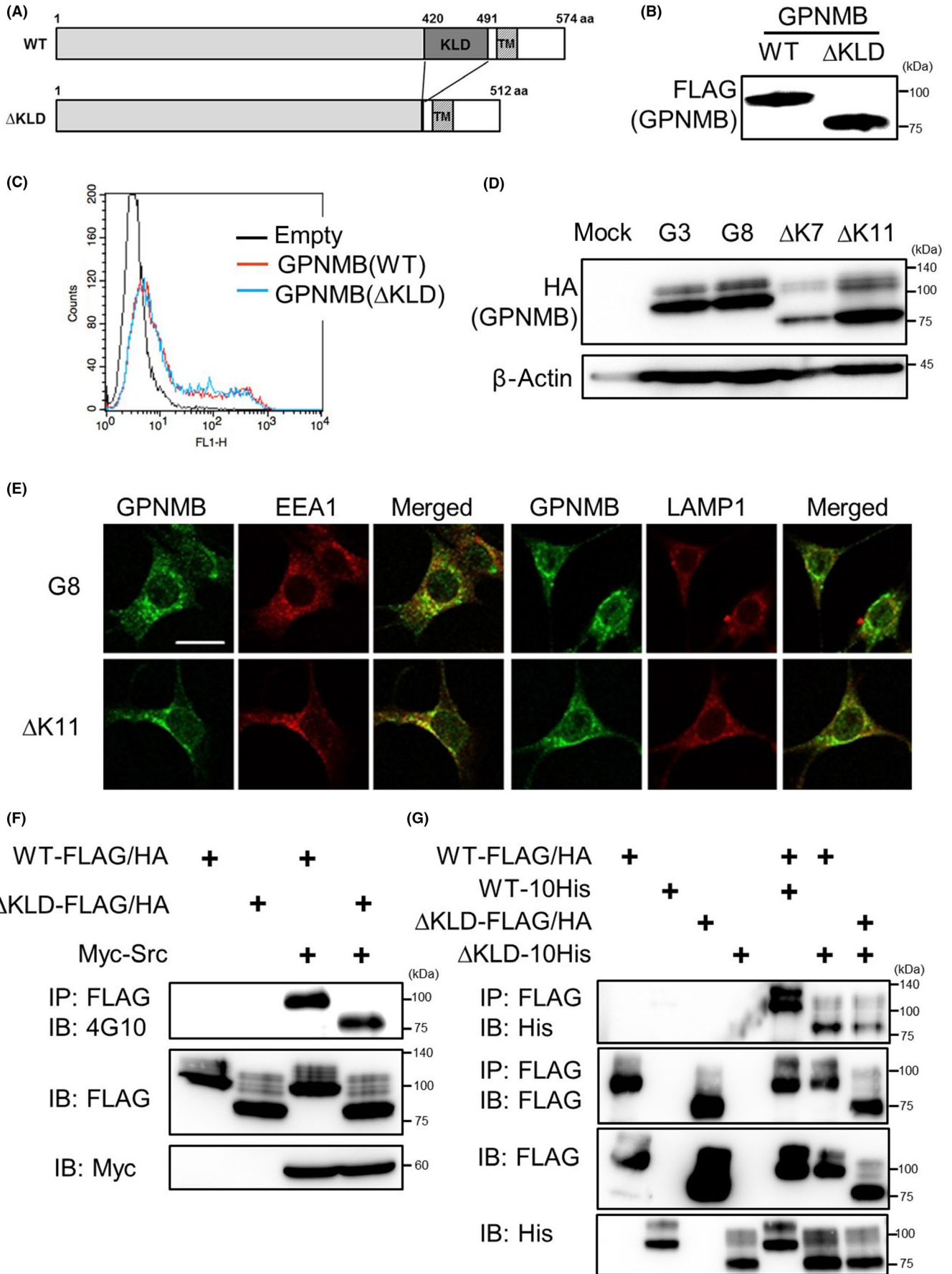


**FIGURE 2** Deletion of the kringle-like domain (KLD) from glycoprotein NMB (GPNMB) does not affect its basic properties. A, 2D scheme of mouse WT GPNMB, and a KLD deletion mutant ( $\Delta$ KLD). TM, transmembrane domain. B, Exogenous expression of GPNMB(WT) and GPNMB( $\Delta$ KLD) in 293T cells. 293T cells were transfected with pCAGIP-GPNMB(WT)-FLAG/HA or pCAGIP-GPNMB( $\Delta$ KLD)-FLAG/HA, and immunoblot analysis for FLAG was carried out to detect GPNMB(WT) and GPNMB( $\Delta$ KLD). C, Detection of cell-surface expression of GPNMB(WT) and GPNMB( $\Delta$ KLD) in 293T cells by flow cytometry. Black line, empty vector control; red line, GPNMB(WT); blue line, GPNMB( $\Delta$ KLD). D, Stably expressing cell lines were established as NMuMG-mock cells (Mock), NMuMG-GPNMB(WT)-FLAG/HA cells (clone 3 [G3] and clone 8 [G8]), and NMuMG-GPNMB( $\Delta$ KLD)-FLAG/HA cells (clone 7 [ $\Delta$ K7] and clone 11 [ $\Delta$ K11]). Detection of exogenous GPNMB protein expression was undertaken by immunoblot analysis for HA.  $\beta$ -actin was used as the loading control. E, Immunofluorescence staining showing the subcellular localization of GPNMB(WT) or GPNMB( $\Delta$ KLD) (green) in G8 and  $\Delta$ K11 cells. Early endosome antigen 1 (EEA1; red) is an endosomal marker and lysosome-associated membrane protein 1 (LAMP1; red) is a lysosomal marker. Scale bar, 20  $\mu$ m. F,G, Tyrosine phosphorylation and oligomer formation of GPNMB. 293T cells were transfected with the indicated plasmids, and immunoprecipitation (IP) was carried out using anti-FLAG Ab, followed by immunoblot (IB) analysis with anti-phosphorylated tyrosine (4G10), anti-FLAG, and anti-Myc Abs to detect Src-induced tyrosine phosphorylation of GPNMB (F), and with anti-His and anti-FLAG Abs to detect oligomer formation of GPNMB (G)

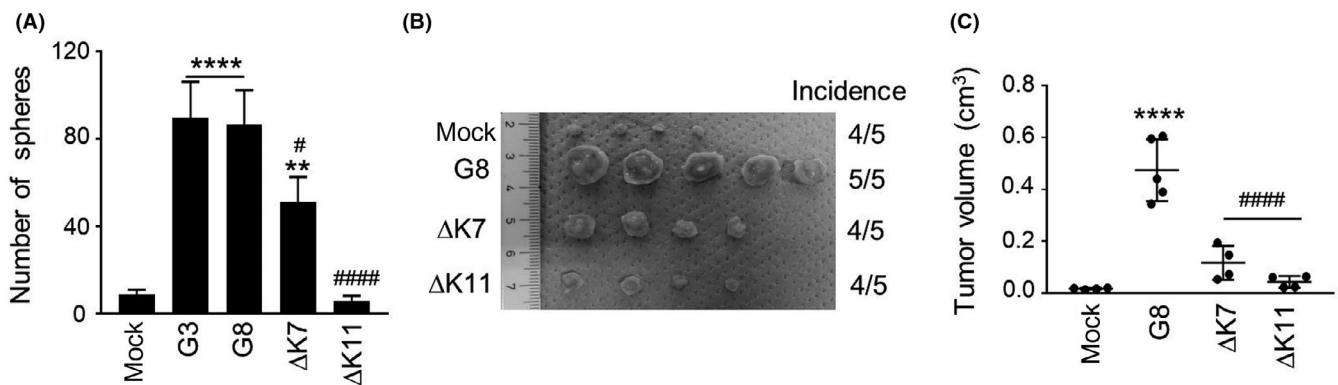


**FIGURE 3** Deletion of the kringle-like domain (KLD) attenuates the tumorigenic ability of glycoprotein NMB (GPNMB). A, Sphere-forming abilities of NMuMG-mock, NMuMG-GPNMB(WT) (G3 and G8), and NMuMG-GPNMB( $\Delta$ KLD) ( $\Delta$ K7 and  $\Delta$ K11) cells were examined. Only spheres larger than 50  $\mu$ m in diameter were counted. Data are presented as mean  $\pm$  SD; n = 3 replicates, representative of 3 independent experiments. \*\* $P$  < 0.01, \*\*\*\* $P$  < 0.0001 (vs mock), # $P$  < 0.05, #### $P$  < 0.0001 (vs G3 and G8), 1-way ANOVA with Tukey multiple comparison test. B,C, Tumor growth abilities of NMuMG-mock, NMuMG-GPNMB(WT) (G8), and NMuMG-GPNMB( $\Delta$ KLD) ( $\Delta$ K7 and  $\Delta$ K11) cells examined by s.c. injection into ICR-*nu/nu* mice. Macroscopic view (B) and measured volumes (C). Data are presented as mean  $\pm$  SD; n = 5 mice. \*\*\*\* $P$  < 0.0001 (vs mock), #### $P$  < 0.0001 (vs G8), 1-way ANOVA with Tukey multiple comparison test

### 3.3 | Kringle-like domain is important in GPNMB-induced tumorigenic potential

To investigate the importance of the KLD in GPNMB-induced tumorigenic growth, we undertook assays of *in vitro* sphere formation and *in vivo* tumor formation. GPNMB( $\Delta$ KLD)-expressing cells showed significantly lower sphere-forming activity than that of GPNMB(WT)-expressing cells (Figure 3A, Table S1). When we injected cells of either NMuMG-GPNMB(WT) or NMuMG-GPNMB( $\Delta$ KLD) s.c. into nude mice, the tumors from the GPNMB( $\Delta$ KLD)-expressing cells were significantly smaller and had a lower incidence than those from the GPNMB(WT) cells (Figure 3B,C, Table S2). These results indicate the essential contribution of the KLD to GPNMB-induced tumorigenic growth in both *in vitro* and *in vivo* systems.

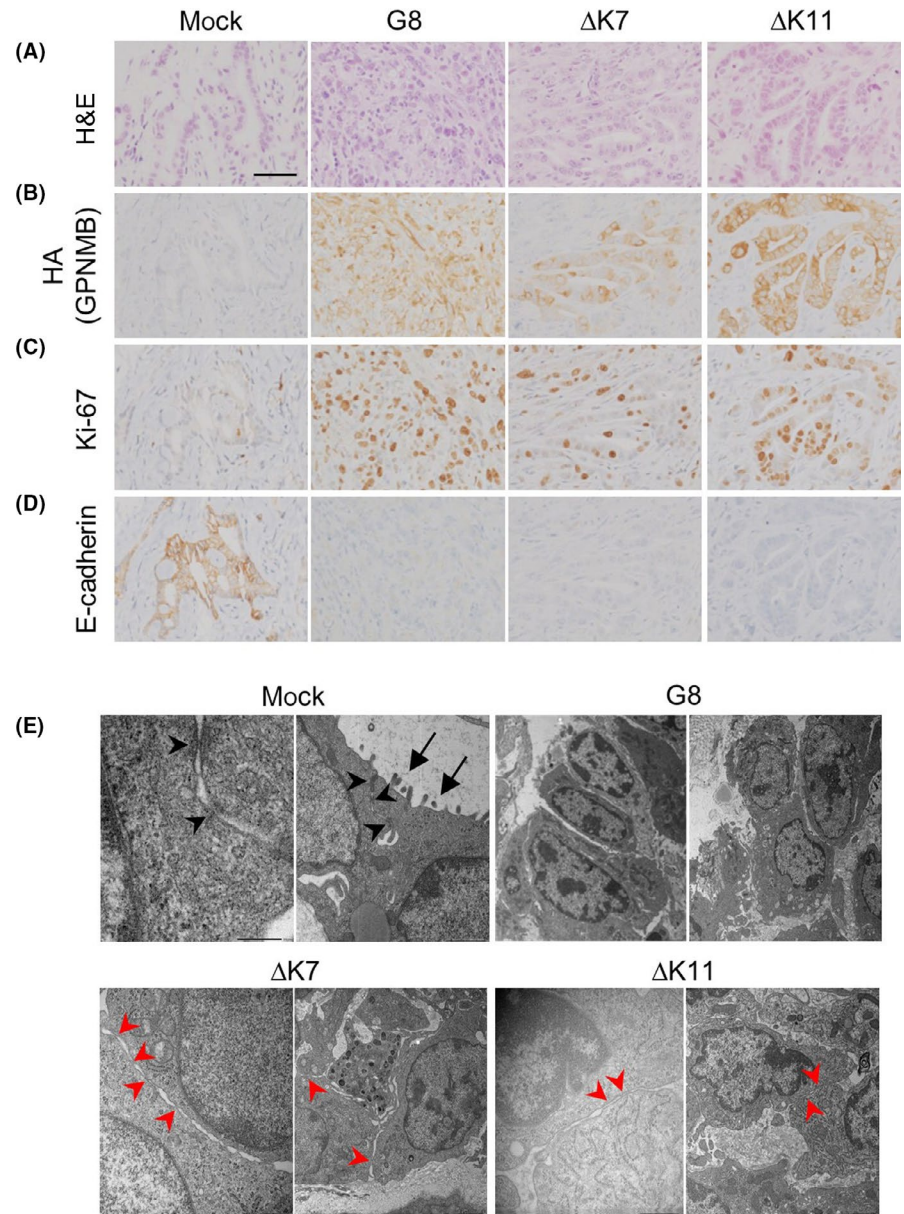
### 3.4 | Deletion of the KLD partially maintains cellular junctions and polarity

We next analyzed each tumor histologically. On H&E staining, tubular structures were observed in the tissue of the NMuMG-mock cells, suggesting their epithelial feature. In contrast, the tumor of

NMuMG-GPNMB(WT) cells consisted of mesenchyme-like cells and no tubule-like structures were seen, as we already reported.<sup>6</sup> To our surprise, the NMuMG-GPNMB( $\Delta$ KLD) cells formed tubular structures, indicating that these cells keep their cell-cell junction and cellular polarity formation (Figure 4A). Additionally, we undertook immunohistochemical staining using anti-HA Ab to detect the expression of either GPNMB(WT) or GPNMB( $\Delta$ KLD) in the tumors. As shown in Figure 4B, most of the tumor cells in the grafts were HA-positive in both cases. These results indicated that the mesenchyme-like tumor cells in the GPNMB(WT) tumor and cells making tubular structures in the GPNMB( $\Delta$ KLD) tumor were derived from NMuMG cells that express either GPNMB(WT) or GPNMB( $\Delta$ KLD). Interestingly, we observed the expression of E-cadherin in the cell-cell border of the tubule-like structures in the mock graft, whereas, like the GPNMB(WT)-expressing cells, the GPNMB( $\Delta$ KLD)-expressing cells lost E-cadherin expression even if tubular structures were generated (Figure 4C). Furthermore, the GPNMB( $\Delta$ KLD) tumor had fewer Ki-67-positive cells (a proliferation marker) than did the GPNMB(WT) tumor (Figure 4D), resulting in slower growth of the grafts *in vivo*.

To examine the cellular junction formation, we used transmission electron microscopy observation to compare the GPNMB(WT) and

**FIGURE 4** Deletion of the kringle-like domain partially maintains cellular junctions and polarity. A-D, Histology of the xenograft tumors shown in Figure 3C was determined by H&E staining (A) and immunohistochemical staining for HA (B), E-cadherin (C), and Ki-67 (D). Scale bar, 50  $\mu$ m. E, Transmission electron microscopic images of the xenografts of NMuMG-mock, NMuMG-GPNMB(WT) (G8), and NMuMG-GPNMB( $\Delta$ KLD) ( $\Delta$ K7 and  $\Delta$ K11) cells as indicated. Arrow, microvilli; black arrowhead, tight junction structure; red arrowhead, tight junction-like structure



GPNMB( $\Delta$ KLD) grafts with the mock grafts. Tight junctions were observed in the mock grafts, whereas none could be observed in the GPNMB(WT) grafts; in addition, no villi could be observed in the GPNMB(WT) grafts, indicating loss of the epithelial feature. However, the GPNMB( $\Delta$ KLD) tumors seemed to have tight junction-like adhesion structures, whereas the GPNMB(WT) tumors did not (Figure 4E). In other words, GPNMB( $\Delta$ KLD) had less disruption of cell polarity, despite not having E-cadherin and mature tight junctions.

### 3.5 | Deletion of the KLD maintains the GPNMB function to suppress E-cadherin expression but impairs its function to activate cellular migration and Wnt/ $\beta$ -catenin signaling

We further examined the phenotypes of GPNMB( $\Delta$ KLD) cells in terms of the induction of EMT. Previously, we reported that enhanced

expression of GPNMB(WT) induces EMT phenotypes in NMuMG cells, such as downregulation of E-cadherin, promotion of cellular migration and invasion, and induction of stem-like properties in breast cancer cells.<sup>6,7</sup> As shown in Figure 5A and 5B, GPNMB( $\Delta$ KLD) induced suppression of E-cadherin, as did GPNMB(WT). However, when we investigated the actin fiber structures, GPNMB(WT) activated stress fiber formation, whereas GPNMB( $\Delta$ KLD) retained the cortical actin fibers (Figure 5C). Furthermore, a Transwell migration assay indicated that GPNMB( $\Delta$ KLD) lacked the cell migration-promoting effect (Figure 5D, Table S3). Taken together, these findings indicate that the deletion of the KLD from GPNMB could impair GPNMB-induced motility even if suppression of E-cadherin was observed by stable expression of GPNMB( $\Delta$ KLD) in NMuMG cells. The molecular mechanism that explains how deletion of the KLD partially impairs EMT and the cell migration-inducing activity of GPNMB has not been fully elucidated yet, but our preliminary examination indicated the impairment

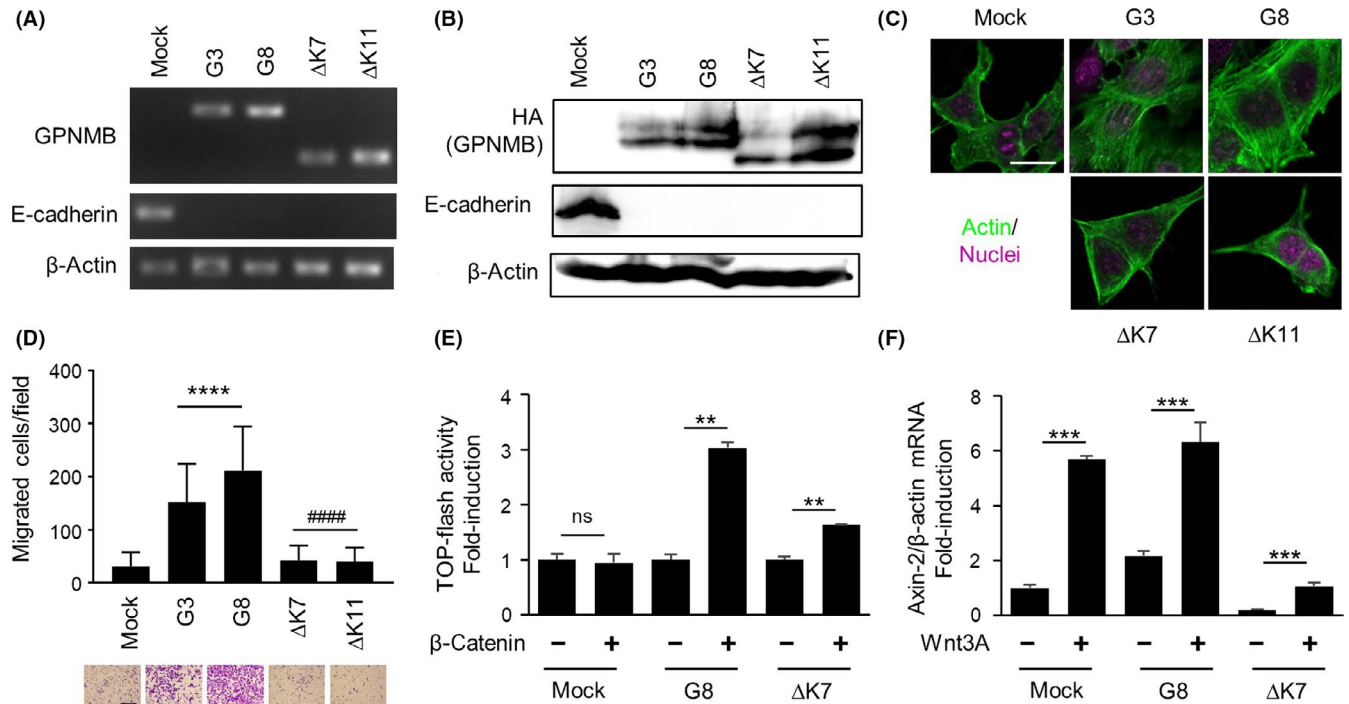


**FIGURE 5** Deletion of the kringle-like domain (KLD) maintains the glycoprotein NMB (GPNMB) function to suppress E-cadherin expression but impairs its function to activate cellular migration and Wnt/β-catenin signaling. A,B, Expressions of GPNMB, E-cadherin, and β-actin in NMuMG-mock, NMuMG-GPNMB(WT) (G3 and G8), and GPNMB(ΔKLD) (ΔK7 and ΔK11) cells were examined by RT-PCR for mRNA (A) and by immunoblot analysis for proteins (B). C, Immunofluorescence staining showing stress fiber formation in NMuMG-mock, NMuMG-GPNMB(WT) (G3 and G8), and NMuMG-GPNMB(ΔKLD) (ΔK7 and ΔK11) cells. Actin (green) was stained using phalloidin (green), and TO-PRO3 (magenta) was used to indicate the nuclei. Scale bar, 20 μm. D, Migration of NMuMG-mock and NMuMG-GPNMB(WT) (G3 and G8), and NMuMG-GPNMB(ΔKLD) (ΔK7 and ΔK11) cells was examined by Transwell migration assay. Data are presented as mean ± SD; n = 3 replicates, representative of 3 independent experiments. \*\*\*\* $P < 0.0001$  (vs mock), ##### $P < 0.0001$  (vs G3 and G8), 1-way ANOVA with Tukey multiple comparison test. Scale bar, 200 μm. E,F, Effects of GPNMB(WT) and GPNMB(DKLD) on Wnt/β-catenin signaling. NMuMG-mock and NMuMG-GPNMB(WT) G8 and NMuMG-GPNMB(ΔKLD) ΔK7 cells were transfected with TOP-flash firefly luciferase reporter and pRL-CMV Renilla luciferase reporter with/without pCAG-GS-β-catenin expressing vectors. Data are presented as mean ± SD; n = 3. \*\* $P < 0.01$ , Student's *t* test. ns, not significant (E). NMuMG-mock and NMuMG-GPNMB(WT) G8 and NMuMG-GPNMB(ΔKLD) ΔK7 cells were treated with Wnt3A conditioned medium or control medium for 3 h and *Axin-2* mRNA was measured by quantitative PCR and normalized to β-actin expression levels. Data are presented as mean ± SD; n = 3. \*\*\* $P < 0.001$ , Student's *t* test (F)

of Wnt/β-catenin signaling detected by TOP-flash reporter assay and *Axin2* mRNA levels (Figure 5E,F). Therefore, supportive effects on Wnt signaling are a possible molecular function of GPNMB KLD.

## 4 | DISCUSSION

This is the first report to identify the importance of the region of amino acids 420-491 in the ECD of mouse GPNMB, a region called the KLD, for the tumorigenic function of GPNMB, such as sphere formation in vivo and tumor growth in vivo (Figure 3). NMuMG-GPNMB(ΔKLD) cells formed tubular structures in the tumor even though the cells did not express E-cadherin, which is involved in the adherence junction. Tight junction-like structures were formed in the tumor of NMuMG-GPNMB(ΔKLD), which was not observed in the NMuMG-GPNMB(WT) tumor (Figure 4A,B). Tight junctions are associated with maintenance of cell polarity; therefore, these results might explain why GPNMB(ΔKLD)-expressing cells partially retain cell polarity when compared with GPNMB(WT).

We previously reported that expression of GPNMB(WT) fully induces EMT in NMuMG cells.<sup>6</sup> In the current study, we have confirmed that overexpression of GPNMB(ΔKLD) suppressed E-cadherin expression at both the mRNA and the protein levels, as well as GPNMB(WT) did (Figure 5A,B). In contrast, GPNMB(ΔKLD) did not induce stress fiber formation nor cell migration (Figure 5C,D). Epithelial-mesenchymal transition is a biological process that allows epithelial cells to harbor mesenchymal phenotypes, which activates cell migration, invasiveness, and resistance to apoptosis, and also contributes to induction of stem-like properties.<sup>25-27</sup> During EMT, dissolution of adherence junction proteins and disruption of the tight junctions lead the cells to lose their cell-cell adhesion and apical-basal polarity, and thus, they become migratory and invasive. However, sometimes it is not easy to divide cancer cells into cells with only epithelial or mesenchymal features, and cells with both epithelial and mesenchymal phenotypes have recently been reported, which is termed partial EMT.<sup>28,29</sup> Although the phenotypes of NMuMG-GPNMB(ΔKLD) are different from those of complete



EMT and partial EMT, it might be a kind of intermediate phenotype between epithelial and mesenchymal, resulting in fewer migratory and tumorigenic abilities.

The point mutant in which the tyrosine residue in hemITAM was altered to phenylalanine, GPNMB(YF), totally lost EMT and stem-like properties inducing activity.<sup>6,7</sup> GPNMB(YF) did not suppress E-cadherin and lacked the promoting effect on cellular migration and sphere and tumor formation,<sup>6</sup> indicating the crucial role of the tyrosine residue in the tumorigenic ability of GPNMB. However, deletion of the KLD impaired the tumorigenic potential, although GPNMB( $\Delta$ KLD) could be phosphorylated by Src when we transiently overexpressed both of them (Figure 2F). Phosphorylation of endogenous GPNMB hemITAM tyrosine in sphere or in tumor could not be directly detected; however, our previous and current findings suggest that this tyrosine phosphorylation is crucial, and additional mechanisms through KLD could be working to fully trigger the tumorigenic function of GPNMB.

The KD is composed of 80 amino acids and 3 intramolecular disulfide bonds to make a typical loop structure. It is thought to be involved in the interactions of proteins, lipids, and small molecules.<sup>30</sup> It is found in proteins such as coagulation factors (prothrombin and coagulation factor XII),<sup>31</sup> proteases (urokinase, plasminogen, plasminogen activator, and serine proteases),<sup>31</sup> growth factors (hepatocyte growth factor),<sup>32</sup> and receptors (RORs and MuSK).<sup>33,34</sup> Both RORs and MuSK contain KD and cysteine rich domain, which is thought to be responsible for Wnt ligand binding, in their ECD. Wnt5A induces ROR1 and ROR2 heterodimerization through KD, and activates chemotaxis and proliferation of leukemia cells.<sup>35</sup> Additionally, MuSK is also involved in the noncanonical Wnt signaling pathway.<sup>36</sup> Recent publications, however, showed that GPNMB is involved in Wnt/ $\beta$ -catenin signaling in glioma, cervical cancer, and breast cancer models.<sup>37-39</sup> These findings bring us one possibility that the KLD of GPNMB is somehow involved in the Wnt signaling pathway and our initial experiments suggested that GPNMB KLD might have some function to support Wnt/ $\beta$ -catenin signaling (Figure 5E,F). Further studies are needed to reveal the mechanism by which the KLD contributes to the tumorigenic function of GPNMB, and identification of the binding partner through this region is essential. The Wnt/PCP pathway must be the focus in studies of the phenotype of GPNMB( $\Delta$ KLD) cell tumors in the future.

Glembatumumab vedotin, or CDX-011, an Ab against GPNMB conjugated with an anticancer drug, has been developed to treat GPNMB-expressing cancers and is in clinical trials for breast cancer and melanoma patients.<sup>5,40-43</sup> This suggests the potential of GPNMB as a therapeutic target. From the findings of this study, we propose that specifically targeting the KLD in the ECD of GPNMB is a possible therapeutic target.

## ACKNOWLEDGMENTS

We thank Flaminia Miyamasu (Medical English Communications Center, University of Tsukuba) for grammatical revision of the manuscript. This research was supported by the Japan Society for

the Promotion of Science (KAKENHI Grant Nos. JP15K29070 and JP17K14981 [to YO] and JP18H02676 [to MK]) and by grants from the Uehara Memorial Foundation (to YO).

## DISCLOSURE

The authors have no conflicts of interest to declare.

## ORCID

Yukari Okita  <https://orcid.org/0000-0002-7279-4634>

Mitsuyasu Kato  <https://orcid.org/0000-0001-9905-2473>

## REFERENCES

- Zhou LT, Liu FY, Li Y, Peng YM, Liu YH, Li J. Gpnmb/osteoactivin, an attractive target in cancer immunotherapy. *Neoplasma*. 2012;59:1-5.
- Maric G, Rose AA, Annis MG, Siegel PM. Glycoprotein non-metastatic b (GPNMB): a metastatic mediator and emerging therapeutic target in cancer. *Onco Targets Ther*. 2013;6:839-852.
- Roth M, Barris DM, Piperdi S, et al. Targeting glycoprotein NMB with antibody-drug conjugate, glembatumumab vedotin, for the treatment of Osteosarcoma. *Pediatr Blood Cancer*. 2016;63:32-38.
- Rose AAN, Biondini M, Curiel R, Siegel PM. Targeting GPNMB with glembatumumab vedotin: current developments and future opportunities for the treatment of cancer. *Pharmacol Ther*. 2017;179:127-141.
- Taya M, Hammes SR. Glycoprotein Non-Metastatic Melanoma Protein B (GPNMB) and cancer: a novel potential therapeutic target. *Steroids*. 2018;133:102-107.
- Okita Y, Kimura M, Xie R, et al. The transcription factor MAFK induces EMT and malignant progression of triple-negative breast cancer cells through its target GPNMB. *Sci Signal*. 2017;10:eaak9397. <https://doi.org/10.1126/scisignal.aak9397>
- Chen C, Okita Y, Watanabe Y, et al. Glycoprotein NMB is exposed on the surface of dormant breast cancer cells and induces stem cell-like properties. *Cancer Res*. 2018;78:6424-6435.
- Lin A, Li C, Xing Z, et al. The LINK-A lncRNA activates normoxic HIF1 $\alpha$  signalling in triple-negative breast cancer. *Nat Cell Biol*. 2016;18:213-224.
- Abdelmagid SM, Barbe MF, Rico MC, et al. Osteoactivin, an anabolic factor that regulates osteoblast differentiation and function. *Exp Cell Res*. 2008;314:2334-2351.
- Selim AA. Osteoactivin bioinformatic analysis: prediction of novel functions, structural features, and modes of action. *Med Sci Monit*. 2009;15:MT19-33.
- Hoashi T, Sato S, Yamaguchi Y, Passeron T, Tamaki K, Hearing VJ. Glycoprotein nonmetastatic melanoma protein b, a melanocytic cell marker, is a melanosome-specific and proteolytically released protein. *FASEB J*. 2010;24:1616-1629.
- Maric G, Annis MG, Dong Z, et al. GPNMB cooperates with neuropilin-1 to promote mammary tumor growth and engages integrin  $\alpha$ 5 $\beta$ 1 for efficient breast cancer metastasis. *Oncogene*. 2015;34:5494-5504.
- Shikano S, Bonkobara M, Zukas PK, Ariizumi K. Molecular cloning of a dendritic cell-associated transmembrane protein, DC-HIL, that promotes RGD-dependent adhesion of endothelial cells through recognition of heparan sulfate proteoglycans. *J Biol Chem*. 2001;276:8125-8134.
- Tomihari M, Hwang SH, Chung JS, Cruz PD Jr, Ariizumi K. Gpnmb is a melanosome-associated glycoprotein that contributes to

- melanocyte/keratinocyte adhesion in a RGD-dependent fashion. *Exp Dermatol.* 2009;18:586-595.
15. Chung JS, Dougherty I, Cruz PD Jr, Ariizumi K. Syndecan-4 mediates the coinhibitory function of DC-HIL on T cell activation. *J Immunol.* 2007;179:5778-5784.
  16. Chung JS, Sato K, Dougherty II, Cruz PD Jr, Ariizumi K. DC-HIL is a negative regulator of T lymphocyte activation. *Blood.* 2007;109:4320-4327.
  17. Chung JS, Bonkobara M, Tomihari M, Cruz PD Jr, Ariizumi K. The DC-HIL/syndecan-4 pathway inhibits human allogeneic T-cell responses. *Eur J Immunol.* 2009;39:965-974.
  18. Tomihari M, Chung JS, Akiyoshi H, Cruz PD Jr, Ariizumi K. DC-HIL/glycoprotein Nmb promotes growth of melanoma in mice by inhibiting the activation of tumor-reactive T cells. *Cancer Res.* 2010;70:5778-5787.
  19. Chung JS, Shiue LH, Duvic M, Pandya A, Cruz PD Jr, Ariizumi K. Sezary syndrome cells overexpress syndecan-4 bearing distinct heparan sulfate moieties that suppress T-cell activation by binding DC-HIL and trapping TGF-beta on the cell surface. *Blood.* 2011;117:3382-3390.
  20. Amalia R, Abdelaziz M, Puteri MU, et al. TMEPAI/PMEPA1 inhibits Wnt signaling by regulating  $\beta$ -catenin stability and nuclear accumulation in triple negative breast cancer cells. *Cell Signal.* 2019;59:24-33.
  21. Okita Y, Kamoshida A, Suzuki H, et al. Transforming growth factor- $\beta$  induces transcription factors MafK and Bach1 to suppress expression of the heme oxygenase-1 gene. *J Biol Chem.* 2013;288:20658-20667.
  22. Shen LT, Chou HE, Kato M. TIF1 $\beta$  is phosphorylated at serine 473 in colorectal tumor cells through p38 mitogen-activated protein kinase as an oxidative defense mechanism. *Biochem Biophys Res Commun.* 2017;492:310-315.
  23. Zheng L, Suzuki H, Nakajo Y, Nakano A, Kato M. Regulation of c-MYC transcriptional activity by transforming growth factor-beta 1-stimulated clone 22. *Cancer Sci.* 2018;109:395-402.
  24. Ho T, Watt B, Spruce LA, Seeholzer SH, Marks MS. The kringle-like domain facilitates post-endoplasmic reticulum changes to Premelanosome Protein (PMEL) oligomerization and disulfide bond configuration and promotes amyloid formation. *J Biol Chem.* 2016;291:3595-3612.
  25. Kalluri R, Weinberg RA. The basics of epithelial-mesenchymal transition. *J Clin Invest.* 2009;119:1420-1428.
  26. Thiery JP, Acloque H, Huang RY, Nieto MA. Epithelial-mesenchymal transitions in development and disease. *Cell.* 2009;139:871-890.
  27. Dongre A, Weinberg RA. New insights into the mechanisms of epithelial-mesenchymal transition and implications for cancer. *Nat Rev Mol Cell Biol.* 2019;20:69-84.
  28. Grigore AD, Jolly MK, Jia D, Farach-Carson MC, Levine H. Tumor Budding: the Name is EMT. Partial EMT. *J Clin Med.* 2016;5:E51. <https://doi.org/10.3390/jcm5050051>
  29. Saitoh M. Involvement of partial EMT in cancer progression. *J Biochem.* 2018;164:257-264.
  30. Lee CH, Park KJ, Sung ES, et al. Engineering of a human kringle domain into agonistic and antagonistic binding proteins functioning in vitro and in vivo. *Proc Natl Acad Sci USA.* 2010;107:9567-9571.
  31. Castellino FJ, Beals JM. The genetic relationships between the kringle domains of human plasminogen, prothrombin, tissue plasminogen activator, urokinase, and coagulation factor XII. *J Mol Evol.* 1987;26:358-369.
  32. Nakamura T, Mizuno S. The discovery of hepatocyte growth factor (HGF) and its significance for cell biology, life sciences and clinical medicine. *Proc Jpn Acad Ser B Phys Biol Sci.* 2010;86:588-610.
  33. Rebagay G, Yan S, Liu C, Cheung NK. ROR1 and ROR2 in human malignancies: potentials for targeted therapy. *Front Oncol.* 2012;2:34.
  34. Saldanha J, Singh J, Mahadevan D. Identification of a Frizzled-like cysteine rich domain in the extracellular region of developmental receptor tyrosine kinases. *Protein Sci.* 1998;7:1632-1635.
  35. Yu J, Chen L, Cui B, et al. Wnt5a induces ROR1/ROR2 heterooligomerization to enhance leukemia chemotaxis and proliferation. *J Clin Invest.* 2016;126:585-598.
  36. Banerjee S, Gordon L, Donn TM, et al. A novel role for MuSK and non-canonical Wnt signaling during segmental neural cell migration. *Development.* 2011;138:3287-3296.
  37. Bao G, Wang N, Li R, Xu G, Liu P, He B. Glycoprotein non-metastatic melanoma protein B promotes glioma motility and angiogenesis through the Wnt/ $\beta$ -catenin signaling pathway. *Exp Biol Med.* 2016;241:1968-1976.
  38. Xu S, Fan Y, Li D, Liu Y, Chen X. Glycoprotein nonmetastatic melanoma protein B accelerates tumorigenesis of cervical cancer in vitro by regulating the Wnt/ $\beta$ -catenin pathway. *Braz J Med Biol Res.* 2018;52:e7567.
  39. Maric G, Annis MG, MacDonald PA, et al. GPNMB augments Wnt-1 mediated breast tumor initiation and growth by enhancing PI3K/AKT/mTOR pathway signaling and  $\beta$ -catenin activity. *Oncogene.* 2019. <https://doi.org/10.1038/s41388-019-0793-7>
  40. Bendell J, Saleh M, Rose AA, et al. Phase I/II study of the antibody-drug conjugate glembatumumab vedotin in patients with locally advanced or metastatic breast cancer. *J Clin Oncol.* 2014;32:3619-3625.
  41. Ott PA, Hamid O, Pavlick AC, et al. Phase I/II study of the antibody-drug conjugate glembatumumab vedotin in patients with advanced melanoma. *J Clin Oncol.* 2014;32:3659-3666.
  42. Yardley DA, Weaver R, Melisko ME, et al. EMERGE: a randomized phase ii study of the antibody-drug conjugate glembatumumab vedotin in advanced glycoprotein NMB-expressing breast cancer. *J Clin Oncol.* 2015;33:1609-1619.
  43. Ott PA, Pavlick AC, Johnson DB, et al. A phase 2 study of glembatumumab vedotin, an antibody-drug conjugate targeting glycoprotein NMB, in patients with advanced melanoma. *Cancer.* 2019;125:1113-1123.

## SUPPORTING INFORMATION

Additional supporting information may be found online in the Supporting Information section at the end of the article.

**How to cite this article:** Xie R, Okita Y, Ichikawa Y, et al. Role of the kringle-like domain in glycoprotein NMB for its tumorigenic potential. *Cancer Sci.* 2019;110:2237-2246. <https://doi.org/10.1111/cas.14076>